

# Structural Analysis of Nanocrystals by 3D Electron Diffraction Tomography

C. A. Corrêa,<sup>a,b</sup> M. Klementová,<sup>b</sup> and L. Palatinus<sup>b</sup>

<sup>a</sup> Charles University, Faculty of Mathematics and Physics, Prague, Czech Republic.

<sup>b</sup> Institute of Physics of the Academy of Sciences of the Czech Republic.

**Abstract.** In this work the structure solution of a nanocrystal of the transition metal silicide  $\text{Ni}_3\text{Si}_2$ , with the diameter of 22 nm, is obtained by combining the electron diffraction tomography with precession electron diffraction. The dynamical and the kinematical refinements are compared, showing that the dynamical refinement is superior to the kinematical refinement, giving more accurate structure model.

## Introduction

The development of nanotechnology demands the understanding of the properties and characteristics, among them the crystal structure, of nano-sized materials. However, sometimes it is difficult or impossible to obtain crystals large enough for single crystal X-ray diffraction experiment, and the properties of nanostructures might be different from the bulk. In this sense the electron diffraction (ED) technique is of great importance because it can be used in the structure analysis of nanocrystals as small as a few tens of nanometers.

Electron diffraction, has been used in structural analysis of nanocrystals since 1949 [Vainshtein, 1956]. However, two major problems have prevented the straightforward use of the technique. First, the difficulty to obtain a complete data set with enough reflections to be used as an input to a software for structure solution. Second, the strong dynamical interactions between electrons and matter. These problems can be partially solved by three-dimensional electron diffraction tomography (EDT) and precession electron diffraction (PED), respectively.

In the three-dimensional electron diffraction tomography the crystal is rotated around an arbitrary axis in small steps and diffraction patterns are collected at each step for the same crystal. Since the angles between the diffraction patterns are known, the reciprocal space can be reconstructed giving additional information about the electron diffraction [Kolb *et al.*, 2007, 2008; Gemmi *et al.*, 2013]. As electrons interact with matter about a 1000 times stronger than X-rays and multiple scattering plays an important role in the diffracted intensities, it is necessary to use the dynamical diffraction theory.

The dynamical diffraction theory considers the influence of the interaction between wave and matter on the diffracted intensities [Dederichs, 1971; Spence and Zuo, 1992]. The dynamical character of the diffraction can be suppressed by using precession electron diffraction [Vincent and Midgley, 1994].

The PED technique consists in the deflection of the incident beam from the optical axis, with a precession angle of a few degrees, making a cone surface with vertex on the sample. The coils after the specimen deflect the beam back to the optical axis, so that the reflections are spots, as can be seen in Figure 1 (left). The result is a diffraction pattern, which has intensities integrated from diffraction conditions over a range of angles  $\alpha$ :  $I_g^{exp} \propto \int_0^{2\pi} I_g(\alpha) d\alpha$  [Vincent and Midgley, 1994; Gjønnes, 1997]. This integration gives intensities closer to kinematical approximation than a standard diffraction pattern, where the PED is not used and only a cross section of each reflection with the Ewald sphere is considered. In the right side of Figure 1 it is shown the range of angles ( $\alpha$ ) used for the integration of the reflection, and the Ewald sphere cutting the reflection, when the PED is not used.

Although EDT and PED allow solving structures *ab initio*, the lack of a general routine to analyze the structures considering the dynamical theory still prevents the wide use of the

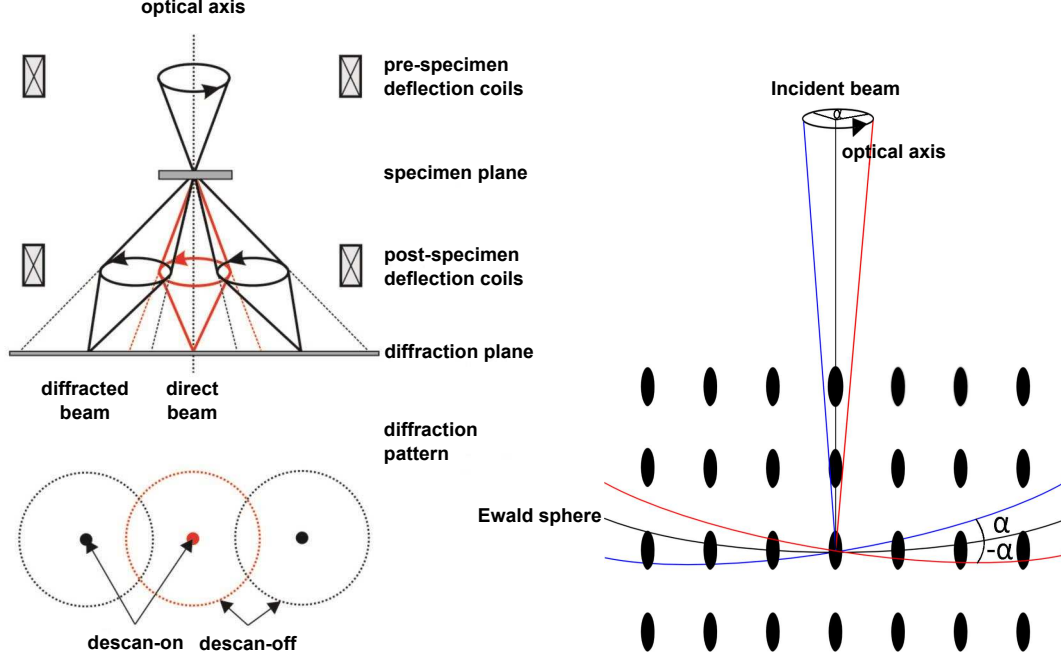


**Figure 1.** Scheme of PED showing the deflected beam forming a cone surface with vertex at the sample (left) and the range where the Ewald sphere sweeps the rods of reflections (right).

technique [Gönnens *et al.*, 1998; Gemmi and Nicolopoulos, 2007; Palatinus *et al.*, 2013]. To our knowledge, the only routine using dynamical refinement for EDT data sets with PED is implemented in the crystallographic software JANA2006 [Petríček *et al.*, 2006, 2014], developed in our laboratory, at the Institute of Physics of the Academy of Sciences of the Czech Republic.

The method of calculation of the dynamical interaction used in JANA2006 is the Bloch-wave method. In this method the intensities are given by the square of the elements of the scattering matrix  $I_i = |S_{i1}|^2$ , where  $\mathbf{S} = e^{2\pi i t \mathbf{A}}$ ,  $t$  is the thickness of the sample and  $\mathbf{A}$  is the structure matrix given by:

$$a_{ij} = \begin{cases} U_{\mathbf{g}_i - \mathbf{g}_j}, & i, j = 1, N_{beams}; i \neq j \\ 2K S_{\mathbf{g}_i}, & i = 1, N_{beams}; i = j \end{cases}$$

Here  $U_{\mathbf{g}}$  is the dynamical structure factor for a given reciprocal lattice vector  $\mathbf{g}$ ,  $K$  is the incident electron wavevector corrected for mean inner potential and  $S_{\mathbf{g}}$  is the excitation error [Spence and Zuo, 1992].

In the present paper, the structure of a single nanocrystal was elucidated using a data set collected with PED and 3D tomography. The kinematical and the dynamical refinements were compared. The sample analyzed is the known phase of the transition metal silicide  $\text{Ni}_3\text{Si}_2$ . The transition metal silicides have been used in micro and nano-sized electronic devices [Reader *et al.*, 1992], and photovoltaics [Klochko *et al.*, 2013] due to their properties such as low electrical resistance, high-temperature stability and high resistance to oxidation.

## Experimental

Samples of nickel silicide nanowires were prepared by chemical vapor deposition (CVD) and were provided by the Institute of Chemical Processes Fundamentals of the AS CR, v.v.i. The diffraction patterns were collected on a transmission electron microscope (TEM) Philips CM120 with a  $\text{LaB}_6$  cathode at acceleration voltage 120 kV. The microscope is equipped with a precession device Nanomegas DigiStar. The images were recorded with a CCD camera Olympus Veleta in  $2048 \times 2048$  pixels and dynamic range of 14 bits.

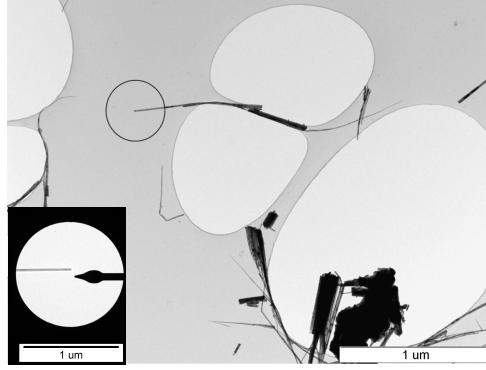


**Figure 2.** Crystal selected for data acquisition. The circle shows the part of the crystal selected for data collection by SAED.

Data collection was performed for a nanowire with the diameter of 22 nm (Figure 2), combining EDT and PED. The precession angle was set to  $1^\circ$ . The nanocrystal was tilted in steps of  $1^\circ$  around the main axis of the sample holder, from  $-52^\circ$  to  $50^\circ$ , and the diffraction patterns collected with 1 s of exposure. Selected area electron diffraction (SAED) was used to collect the data from a smaller part of the nanowire, shown in the square in Figure 2 (left, bottom).

The software PETS [Palatinus, 2011] was used for locating peaks in the images with 70% of completeness for  $d=0.70 \text{ \AA}$  of resolution. PETS was also used to refine the angle between the rotation axis and the horizontal axis, using a methodology similar to the one developed by Kolb et al. [Kolb et al., 2009; Palatinus et al., 2011]. The unit cell was identified in the graphical interface of JANA2006 and the orientation matrix was refined and used for predicting the positions of the peaks, which were integrated by PETS. The integrated intensities result in a list of reflections suitable for structure solution, which was done by charge flipping with SUPERFLIP [Palatinus and Chapuis, 2007], interfaced from JANA2006. The refinement was performed considering the kinematical and the dynamical theories. For the dynamical refinement, each frame has to be fitted individually and the reflections are not averaged by symmetry. Hence, the number of observed intensities is higher for the dynamical refinement than for the kinematical refinement, as can be seen in Table 2. Also, since the dynamical refinement is very sensitive to thickness and orientation of the incident beam in relation to the crystal lattice, both parameters were optimized prior to the structure refinement.

## Previous results and discussion

The structure of  $\text{Ni}_3\text{Si}_2$  was published in 1961 [Pilström, 1961], with unit cell identification from powder diffraction data (Table 1) and solution from single crystal data in the space group  $Cmc2_1$ .

The unit cell of the nanowire reported here was identified as orthorhombic (Table 1), Laue class  $mmm$  with  $R_{int}(\text{obs/all})=28.22/28.35\%$ . The differences in the unit cell parameters, compared to the published parameters, are within the accuracy of the method. From the extinction conditions present in the zones  $0kl$  and  $hk0$ , the possible space groups were  $Cmcm$ ,  $Cmc2_1$  and  $C2cm$ . The structure could be solved and refined in the centrosymmetric space group  $Cmcm$  with good convergence (Table 2). The structure presented here is consistent with the published structure, except for the space group.

Since Pilström [1961] describes the structure in space group  $Cmc2_1$ , we transformed our solution to this space group and refined it to verify the space group assignment.

First, the residue values were compared for the kinematical and for the dynamical refinements, as can be seen in Table 2. For the kinematical refinement, the noncentrosymmetric model has lower values. However, when the dynamical refinement is performed, both models have basically the same residue values (Table 2).

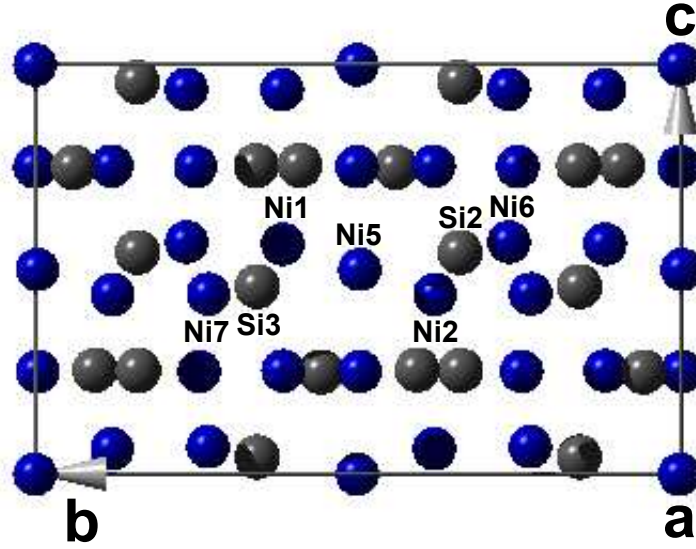


**Figure 3.** Model  $Cmc2_1$  from the dynamical refinement, view along **a**.

Second, the atomic displacements from the symmetric position of atoms in model  $Cmc2_1$ , which were equivalent by the center of symmetry in model  $Cmcm$ , were compared. From 10 independent atoms in the model  $Cmcm$ , 3 atoms split positions when the structure is transformed to  $Cmc2_1$ . The 3 pairs of atoms have small shift from the symmetric position. For example, for models from the dynamical refinement, the atom Ni5, which was positioned in the center of symmetry with atomic coordinates (0.5,0.5,0.5), was shifted to position (0.5,0.4981(6),0.4983(9)) (Figure 3). For models from the kinematical refinement this shift was from position (0.5,0.5,0.5) to (0.5,0.4914(10),0.5041(18)).

The small displacement from the symmetric position indicates the possibility of the model to be centrosymmetric, which is supported by the residue values from the dynamical refinement. In this case the space group was decided to be centrosymmetric,  $Cmcm$ .

**Table 1.** Unit cell parameters obtained by ED and from the published structure [Pilström, 1961].

Parameter	Electron diffraction	Published structure
a (Å)	12.5207	12.229
b (Å)	11.0491	10.805
c (Å)	7.0209	6.924
Crystal system	Orthorhombic	Orthorhombic
$V_{UC}$ (Å <sup>3</sup> )	971.2886	914.8982
Z	16	16
Density (g cm <sup>-3</sup> )	6.3527	6.7421

**Table 2.** Residue values for space groups  $Cmc2_1$  and  $Cmcm$ .

Parameter	$Cmc2_1$		$Cmcm$	
Refinement	Kinematical	Dynamical	Kinematical	Dynamical
$R_{obs}(\%)/R_{all}(\%)$	19.23/21.32	6.80/10.10	21.73/23.13	6.80/10.10
$wR_{obs}(\%)/wR_{all}(\%)$	20.68/20.76	6.44/6.68	24.78/24.80	6.46/6.70
$GOF_{obs}(\%)/GOF_{all}(\%)$	10.72/10.26	2.55/2.13	14.44/13.98	2.55/2.13
Observed reflections	926	1650	515	1657
Parameters refined	44	147	28	131

In Table 2 it is also possible to compare the kinematical and the dynamical refinements. For example, when the dynamical refinement is used for the model  $Cmcm$ , the residue value  $R$  decreased from 21.73% to 6.80%, and the weighted residue value  $wR$  decreased from 24.78% to 6.46%. These decreases show the considerable improvement and therefore, the superiority of the dynamical refinement.

## Conclusion

The use of three-dimensional electron diffraction tomography and precession electron diffraction have been used for structure analysis of a single nanocrystal of  $Ni_3Si_2$  with a diameter of 22 nm, giving reliable structure solution. The kinematical and the dynamical refinements were compared for the structure of the single nanocrystal. The use of the dynamical refinement results in more accurate model, showing that it is superior to the kinematical refinement. The structure of  $Ni_3Si_2$  was decided to have centrosymmetric space group  $Cmcm$ , in disagreement to the published structure, which was only possible because the dynamical refinement was used.

**Acknowledgments.** The authors thank the Institute of Chemical Processes Fundamentals of the AS CR, v.v.i., for the preparation of the sample.

## References

- Dederichs, P.H., Dynamical Diffraction Theory, Kernforschungsanlage Jülich, Institut für Festkörperforschung, 1971.
- Gemmi, M., S. Nicolopoulos, Structure solution with three-dimensional sets of precessed electron diffraction intensities, *Ultramicroscopy* 107, 483–494, 2007.
- Gemmi, M., A. Galanis, F. Karavassili, P.P. Das, M. Calamiotou, A. Gantis, M. Kollia, I. Margiolaki, and S. Nicolopoulos, Structure determination of nano-crystals with precession 3d electron diffraction tomography in the transmission electron microscope, *Microscopy and Analysis* 27(2), 24–29, 2013.
- Gjønnes, K., On the integration of electron diffraction intensities in the Vicent–Midgley precession technique, *Ultramicroscopy*, 69, 1–11, 1997.
- Gjønnes, L., Y. Cheng, B.S. Berg, and V. Hansen, Corrections for multiple scattering in integrated electron diffraction intensities. Application to determination of structure factors in the [001] projection of  $Al_mFe$ , *Acta Crystallographica* A54, 102–119, 1998.
- Klochko, N.P., G.S. Khrypunov, V.R. Kopach, I.I. Tyukhov, K.S. Klepikova, M.V. Kirichenko, and V.M. Lyubov, Ultrasound assisted nickel plating and silicide contact formation for vertical multi-junction solar cells, *Solar Energy* 98, 384–391, 2013.
- Kolb, U., T. Gorelik, C. Kübel, M.T. Otten, D. Hubert, Towards automated diffraction tomography: Part I — Data acquisition. *Ultramicroscopy* 107, 507–513, 2007.
- Kolb, U., T. Gorelik, M.T. Otten, Towards automated diffraction tomography. Part II — Cell parameter determination. *Ultramicroscopy*, 108, 763–772, 2008.
- Kolb, U., T. Gorelik, E. Mugnaioli, Automated diffraction tomography combined with electron precession: a new tool for *ab initio* nanostructure analysis. *Mater. Res. Soc. Symp. Proc.*, 1184, 2009, Warrendale PA, USA, GG01-05.
- Palatinus, L., G. Chapuis, SUPERFLIP — a computer program for the solution of crystal structures by charge flipping in arbitrary dimensions, *Journal of Applied Crystallography*, 40, 786–790, 2007.
- Palatinus, L., M. Klementová, V. Dřínek, M. Jarošová, and V. Petříček, An incommensurately modulated structure of  $\eta'$ -phase of  $Cu_{3+x}Si$  determined by quantitative electron diffraction tomography, *Inorganic Chemistry*, 50, 3743–3751, 2011.
- Palatinus, L., PETS — program for analysis of electron diffraction data, Institute of Physics, Prague, Czech Republic, 2011.
- Palatinus, L., J. Damien, P. Cuvillier, M. Klementová, W. Shinkler, and L.D. Marks, Structure refinement from precession electron diffraction data, *Acta Cryst.* A69, 171–188, 2013.
- Petříček, V., M. Dušek, and L. Palatinus, The crystallographic computing system JANA2006, Institute of Physics, Prague, Czech Republic, 2006.
- Petříček, V., M. Dušek, and L. Palatinus, The crystallographic computing system JANA2006:General features, *Z. Kristallgr.* 229(5), 345–352, 2014.

- Pilström, G., The crystal structure of  $Ni_3Si_2$  with some notes on  $Ni_5Si_2$ , *Acta chemica scandinavica*, 15, 4, 893–902, 1961.
- Reader, A.H.; A.H. van Ommen, P.J.W. Weijs, R.A.M. Wolters, and D.J. Oostra, Transition metal silicides in silicon technology, *Reports on Progress in Physics*, 56, 11, 1397–1467, 1992.
- Spence, J.C.H., and J.M. Zuo, Electron Diffraction, *Plenum Press, New York*, 1992.
- Vainshtein, B.K., Structure analysis by electron diffraction, Institute of crystallography of the academy of sciences of the USSR, Moscow, serie X del nuovo cimento, 4, 773–797, 1956.
- Vincent, R., and P.A. Midgley, Double conical beam-rocking system for measurement of integrated electron diffraction intensities, *Ultramicroscopy*, 53, 271–282, 1994.